

# Optofluidic Assembly of Microdisk Lasers on a Silicon Chip

Aaron T. Ohta, Ming-Chun Tien, Kyoungsik Yu, Steven L. Neale, and Ming C. Wu

Dept. of Electrical Engineering and Computer Sciences, Univ. of California, Berkeley, CA 94720, USA  
Contact e-mail: aohta@eecs.berkeley.edu

**Abstract:** A room-temperature optofluidic assembly process to integrate III-V microdisk lasers on a silicon chip is demonstrated. The assembly is accomplished using lateral-field optoelectronic tweezers, which achieves an unoptimized placement accuracy of approximately  $\pm 0.25 \mu\text{m}$ .

## 1. Introduction

Silicon photonics enables intimate integration of CMOS electronics and optoelectronic components such as modulators and photodetectors. However, on-chip optical sources are needed for most applications. Thus, the challenge is to integrate semiconductor lasers with CMOS circuits on a silicon wafer. Silicon Raman lasers have been demonstrated [1, 2], but external optical pumps are required. Heteroepitaxy can grow compound semiconductor lasers directly on Si, but the growth temperature ( $> 400^\circ\text{C}$ ) is usually too high for post-CMOS processing [3]. To circumvent this issue, low temperature ( $300^\circ\text{C}$ ) wafer bonding techniques have been used to integrate hybrid AlGaInAs/Si lasers on silicon wafers [4]. However, integrating lasers on fully-processed CMOS wafers presents additional challenges as the silicon bonding surfaces are buried underneath up to ten layers of electrical interconnects. To address this issue, we propose a novel optofluidic assembly technique to integrate thin ( $0.2 \mu\text{m}$ ), compact ( $5$  to  $10 \mu\text{m}$  in diameter) III-V microdisk lasers on patterned Si wafers. The room-temperature optofluidic assembly process is realized using lateral-field optoelectronic tweezers (LOET), and enables the integration of compound semiconductor components with CMOS circuits.

## 2. Microdisk Fabrication and Assembly

The microdisks consist of an InGaAs/InGaAsP multiple-quantum-well structure, sandwiched by two larger-bandgap optical confinement layers, for a total thickness of  $0.2 \mu\text{m}$  [5]. Microdisks with diameters of  $5$  and  $10 \mu\text{m}$  are fabricated from an InP epitaxial wafer, and suspended in ethanol for assembly by LOET.

Microdisk lasers are assembled on silicon pedestals using LOET (Fig. 1a). The LOET is directly fabricated on a Si wafer. Interdigitated electrodes consisting of a  $100\text{-nm}$ -thick aluminum layer, topped by  $0.8 \mu\text{m}$  of amorphous silicon (a-Si) are deposited on a patterned Si substrate. The  $3\text{-}\mu\text{m}$ -diameter silicon pedestals are centered in the  $5\text{-}\mu\text{m}$ -wide gaps between the LOET electrodes.

The microdisk assembly procedure is shown in Figure 1b. The LOET electrodes create an optically-induced dielectrophoretic force, which is controlled by voltage applied across the electrodes and the position of optical patterns on the light-sensitive a-Si layer [6]. The highest forces are in the illuminated areas near the electrode edges (Fig. 1c). Microdisks are attracted to illuminated areas, and self-align in the gap between the electrodes (Fig. 2a, b). The optical patterns allow transportation of the microdisks along the length of the electrodes using an applied AC voltage of  $1$  to  $10 \text{ Vpp}$  at  $200 \text{ kHz}$ . Once the disks are aligned over a pedestal, the applied voltage is increased to  $20 \text{ Vpp}$  to hold the disks in place as the solution dries (Fig. 2c, d). Ethanol is used to minimize surface tension forces during drying. After drying, the a-Si layer is removed by  $\text{XeF}_2$  etching at  $40^\circ\text{C}$ , so that the a-Si does not interfere with the optical mode of the microdisk. Subsequent SEM images show that the disks with an accuracy of approximately  $\pm 0.25 \mu\text{m}$  (Fig. 2e). This can be further improved by optimizing the optical imaging system.

## 3. Microdisk Laser Measurements

The assembled microdisk lasers are optically pumped by  $0.5\text{-}\mu\text{s}$  pulses with a  $20\text{-kHz}$  repetition rate ( $1\%$  duty cycle) using a  $780\text{-nm}$  diode laser. At room temperature, the  $5\text{-}$  and  $10\text{-}\mu\text{m}$ -diameter microdisks achieve single-mode lasing at wavelengths of  $1558.7 \text{ nm}$  and  $1586 \text{ nm}$ , at threshold pump powers of  $0.85 \text{ mW}$  and  $2.5 \text{ mW}$ , respectively (Fig. 3a). The saturation of the laser output power is due to excess heating of the microdisk. Thermal annealing was performed to improve the microdisk contact to the pedestal, increasing thermal conduction. After annealing, the maximum laser output power increases, indicating improved thermal conduction (Fig. 3b). However, threshold power also increases, due to non-ideal annealing conditions, which are currently being optimized.

[1] O. Boyraz and B. Jalali, *Optics Express* **12**, pp. 5269-5273, 2004.

[2] H. S. Rong, R. Jones, A. S. Liu, O. Cohen, D. Hak, A. Fang, and M. Paniccia, *Nature* **433**, pp. 725-728, 2005.

[3] G. Balakrishnan, et al., *IEEE Journal of Selected Topics in Quantum Electronics* **12**, pp. 1636-1641, 2006.

[4] H. Park, A. W. Fang, S. Kodama, and J. E. Bowers, *Optics Express* **13**, pp. 9460-9464, 2005.

[5] M.-C. Tien, et al., *Conference on Lasers and Electro-Optics (CLEO)*, 2008.

[6] A. T. Ohta, et al., *IEEE Journal of Selected Topics in Quantum Electronics* **13**, pp. 235-243, 2007.

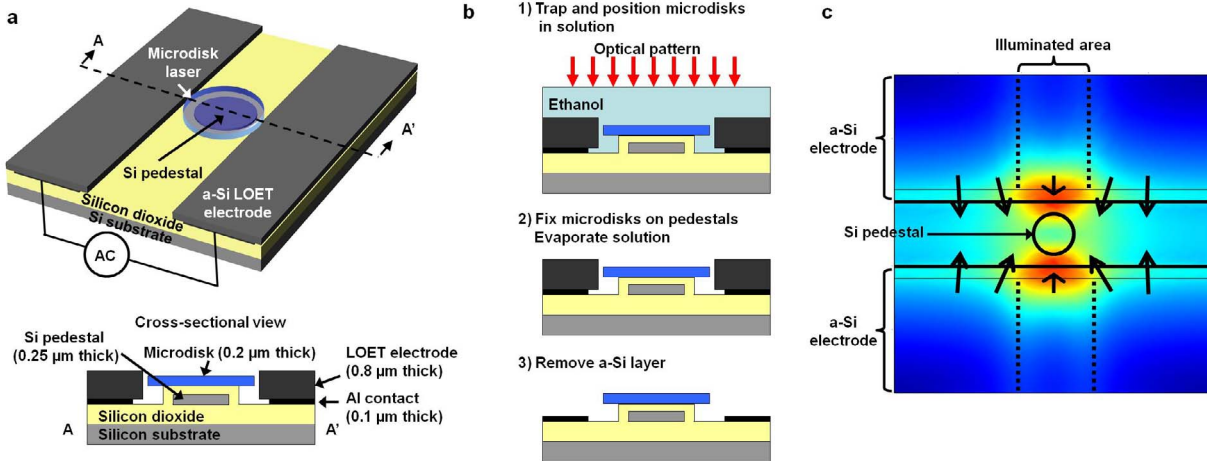


Fig. 1. (a) Schematic of integrated lateral-field optoelectronic tweezers (LOET) for microdisk laser assembly. The integrated LOET electrodes allow optical patterns to control the assembly of III-V microdisks on silicon pedestals. (b) Experimental procedure: microdisks in ethanol are aligned over the pedestals using optical patterns, with a low (1 to 10 Vpp) applied voltage. The voltage is increased to 20 Vpp to fix the disk to the pedestal, followed by evaporation of the solution. The amorphous silicon electrodes are removed by dry etching so they do not interfere with the optical mode of the microdisk. (c) Finite-element simulation of the electric field profile across the LOET electrodes. The arrows show the direction of the optically-induced force.

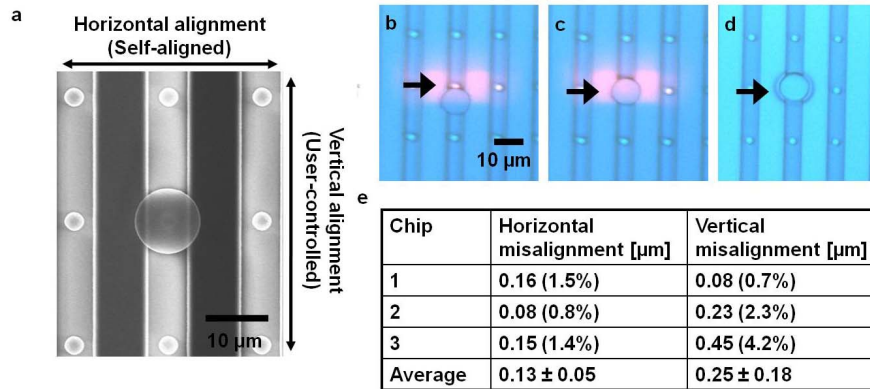


Fig. 2. Assembly of III-V microdisks onto 3- $\mu\text{m}$ -diameter silicon pedestals using lateral-field optoelectronic tweezers. (a) An assembled 10- $\mu\text{m}$ -diameter microdisk. (b-d) Assembly of a 10- $\mu\text{m}$ -diameter microdisk. (b) The initial position of the microdisk. The optical trapping pattern, generated by a computer projector, is visible as a red rectangle. The microdisk is attracted towards the trapping pattern by optically-induced dielectrophoretic force. The target Si pedestal for assembly is indicated by the arrow. (c) The microdisk is positioned over the target Si pedestal. The trapping force is then increased to immobilize the disk on the substrate. (d) The assembled microdisk remains in place after the liquid solution has dried. (e) Alignment accuracy of assembled microdisks on three separate chips. The horizontal alignment is achieved by a self-alignment of the disks across the electrode gap. Vertical alignment is achieved by user control of the optical pattern.

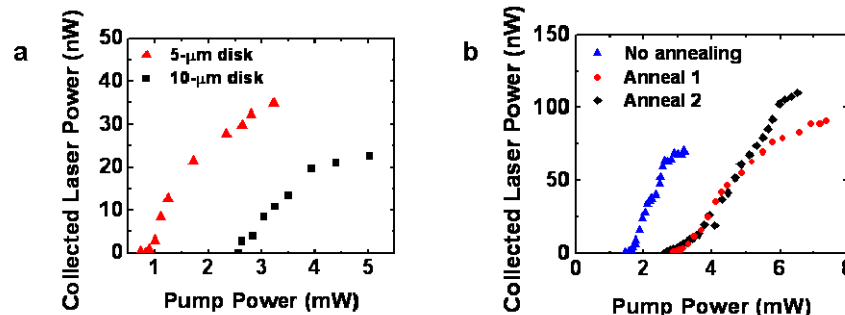


Fig. 3. (a) Peak laser power versus peak pump power. The threshold pump powers for 5- and 10- $\mu\text{m}$ -diameter disks are 0.85 mW and 2.5 mW, respectively. The actual optical power is higher since we are collecting only scattered light from the top of the disk. The 5- $\mu\text{m}$ -diameter microdisk laser has a lower threshold pump power due to the smaller optical mode volume. (b) Improved laser output from thermal annealing. The thermal annealing was performed on a different 5- $\mu\text{m}$  microdisk laser from the data in Fig. 4a; thus, the initial threshold power is slightly higher (1.9 mW). The maximum output power of a 5- $\mu\text{m}$  microdisk laser is improved by annealing for 300°C for 5 hours (Anneal 1), or 300°C for 5 hours, followed by another anneal at 350°C for 5 hours (Anneal 2). After annealing, the maximum output power is increased by 30% and 57% for annealing conditions 1 and 2, respectively.